Thrombospondin-1 (TSP1)–Null and TSP2-Null Mice Exhibit Lower Intraocular Pressures

Ramez I. Haddadin,[1] Dong-Jin Oh,[1] Min Hyung Kang,[1] Guadalupe Villarreal Jr,[1] Ja-Heon Kang,[2] Rui Jin,[3] Haiyan Gong,[3] and Douglas J. Rhee[1]

Purpose. Thrombospondin-1 (TSP1) and TSP2 are matricellular proteins that have been shown to regulate cytoskeleton, cell adhesion, and extracellular matrix remodeling. Both TSP1 and TSP2 are found in the trabecular meshwork (TM). In cadaver eyes with primary open-angle glaucoma (POAG), TSP1 is increased in one third of patients. We hypothesized that TSP1 and TSP2 participate in the regulation of intraocular pressure (IOP).

Methods. IOPs of TSP1-null, TSP2-null mice, and their corresponding wild-type (WT) mice were measured using a commercial rebound tonometer. Fluorophotometric measurements assessed aqueous turnover. Central corneal thickness (CCT) was measured by optical coherence tomography. Iridocorneal angles were examined using light microscopy (LM), immunofluorescence (IF), and transmission electron microscopy (TEM).

Results. Average IOPs of TSP1-null and TSP2-null mice were 10% and 7% less than that of the corresponding WT mice, respectively. CCTs were 6.5% less in TSP1-null mice ($P < 0.05$) and 1.1% less in TSP2-null mice ($P > 0.05$). Fluorophotometric measurements suggest that aqueous turnover rates in TSP1-null and TSP2-null mice are greater than those of WT mice. LM of the TSP1-null and TSP2-null iridocorneal angles reveals morphology, which is indistinguishable from that of their corresponding WTs. IF revealed possible concurrent underexpression of TSP2 in TSP1-null mice and of TSP1 in TSP2-null mice. TEM revealed larger collagen fibril diameters in TSP1-null and TSP2-null mice compared with WTs.

Conclusions. TSP1-null and TSP2-null mice have lower IOPs than their WT counterparts. The rate of aqueous turnover suggests that the mechanism is enhanced outflow facility. An alteration in the extracellular matrix may contribute to this finding. (*Invest Ophthalmol Vis Sci.* 2012;53:6708–6717) DOI: 10.1167/iovs.11-9013

Glaucoma is the leading cause of irreversible blindness worldwide.[1] Elevated intraocular pressure (IOP) is a major risk factor for glaucoma. The relatively elevated IOP of open-angle glaucoma is caused by impaired aqueous drainage through the trabecular meshwork (TM) (i.e., conventional pathway).[2] Although not all of the physiologic processes responsible for the regulation of TM and ciliary body (CB) drainage are known, extracellular matrix (ECM) turnover is at least one contributory factor.[3–5] The mechanisms regulating the deposition and turnover of the ECM are not fully understood.

Matricellular proteins are a group of extracellular proteins that modulate cellular interactions with ECM during embryogenesis and in adult tissues that continue to undergo remodeling.[6] The family includes SPARC (secreted protein, acidic and rich in cysteine), thrombospondin-1 (TSP1) and TSP2, tenascin C and X, SC1/hevin, and osteopontin. A number of these matricellular proteins are widely expressed in ocular tissues including cornea, lens, retina, vitreous, aqueous, and TM, playing specific roles in each tissue.[7–15]

TSP1 and TSP2 are matricellular proteins that have been shown to regulate cytoskeleton, cell adhesion, and ECM remodeling.[7] Both TSP1 and TSP2 are found in the TM; TSP1 is expressed throughout the TM, with a predominance in the juxtacanalicular connective tissue (JCT) region, whereas TSP2 is more concentrated in the uveal meshwork.[14] TSP1 has been implicated in the pathogenesis of glaucoma because its expression is increased in one third of patients with primary open-angle glaucoma (POAG).[16] Consistent with this correlation are the findings that TSP1 expression is increased in situations of fibrosis, wound healing, and other circumstances in which there is significant matrix production.[14,17,18]

The creation of mice deficient in various matricellular proteins has also helped investigate their potential role in IOP regulation.[6] We have previously shown that the prototypical matricellular protein, SPARC, is highly expressed throughout the TM and particularly within the JCT region.[12] SPARC is one of the most highly expressed genes by TM cells[15] at rest and following mechanical stretch.[20] SPARC-null mice exhibit lower IOPs compared with that of their wild-type counterparts, which is the result of enhanced aqueous outflow and not the result of an artifact of central corneal thickness (CCT).[19]

The TSP1-null mouse phenotype includes reduced dermal matrix, thoracic kyphosis, hyperplasia of various epithelial cells, and pulmonary inflammation. Culture of TSP1-null cell isolates revealed one eighth the amount of active TGF-β1.[21] The TSP2-null mouse phenotype includes fragile skin, lax tendons, abnormal collagen fibrils, accelerated skin wound healing, increased bone density, and a bleeding diasthesis.[22–25]

From the [1]Department of Ophthalmology, Massachusetts Eye and Ear Infirmary, Harvard Medical School, Boston, Massachusetts; the [2]Department of Ophthalmology, Kyung Hee University Hospital at Gangdong, College of Medicine, Kyung Hee University, Seoul, Korea; and the [3]Department of Ophthalmology, Boston University School of Medicine, Boston, Massachusetts.

Supported in part by National Eye Institute Grants EY 019654-01 and EY 014104 (Massachusetts Eye and Ear Infirmary Core Grant), Fight for Sight (RIH), Research to Prevent Blindness, Massachusetts Lions Eye Research Foundation, and American Glaucoma Society.

Submitted for publication November 3, 2011; revised July 31 and August 16, 2012; accepted August 16, 2012.

Disclosure: **R.I. Haddadin**, None; **D.-J. Oh**, None; **M.H. Kang**, None; **G. Villarreal Jr**, None; **J.-H. Kang**, None; **R. Jin**, None; **H. Gong**, None; **D.J. Rhee**, None

Corresponding author: Douglas J. Rhee, Department of Ophthalmology, Massachusetts Eye and Ear Infirmary, 243 Charles Street; Boston, MA 02114; DougRhee@aol.com.

Many of these findings, however, are limited to specific tissues, and the effects of TSP1 and TSP2 in the TM have yet to be determined. Given our findings in SPARC-null mice, we hypothesized that TSP1 and TSP2 participate in the regulation of IOP. We tested our hypothesis by comparing the IOP, CCT, and aqueous fluorescein dye clearance of TSP1-null, TSP2-null, and their corresponding wild-type (WT) mice. We subsequently investigated any differences evident by light microscopy (LM), immunofluorescence (IF), and transmission electron microscopy (TEM).

Materials and Methods

Animal Husbandry

All experiments were performed in compliance with the ARVO Statement for the Use of Animals in Ophthalmic and Vision Research. TSP1-null and TSP2-null mice were previously generated,[25,26] and each strain was compared with its own background strain. TSP1-null mice were backcrossed onto a C57BL/6 background for at least eight generations; and the WT strain used was C57BL/6. TSP2-null mice were created from a C57BL/6 × 129/SvJ background, which was the WT strain used. All four strains were obtained from The Jackson Laboratory (Bar Harbor, ME). Each strain of mice was bred independently and genotyped to confirm homozygosity. Briefly, DNA was isolated using a commercial kit including proteinase, and DNA purification reagents (Qiagen, Germantown, MD). PCR was performed with 40 cycles at the following temperatures: denaturation at 95°C for 30 seconds, annealing at 60°C for 30 seconds, and polymerization at 72°C for 1 minute, with an additional 5-minute extension for polymerization at the end of the last cycle. The amplified DNA products were analyzed on 1.5% of agarose gel. The primer sequences used for genotyping of TSP1-null and TSP2-null mice were obtained online from The Jackson Laboratory (www.jax.org). Electron microscopy and immunofluorescence were performed at a later date using different mice. TSP1-null mice were obtained from Sharmila Masli (Schepens Eye Research Institute, Boston, MA) and C57BL/6 wild-type mice were obtained from Charles River Laboratories International (Wilmington, MA). TSP2-null mice were obtained from Jack Lawler (Beth Israel Deaconess Medical Center, Boston, MA) with the corresponding wild-type strain, FVB/N.

All animals used in this experiment were born in the Massachusetts Eye and Ear Infirmary animal facility, fed without restriction, and housed in clear plastic rodent cages under 12/12-hour light–dark cycles (on 7:00 AM, off 7:00 PM) at 21°C. Animal ages at the time of experimentation were 7 to 11 weeks with temporal and age-matching between WTs and TSP-null mice to within 1 week.

Measurement of IOP

Our IOP measurements were performed as previously described.[19] Briefly, the mice were anesthetized by intraperitoneal (IP) injection of a ketamine/xylazine mixture (100 mg/kg and 9 mg/kg, respectively; Phoenix Pharmaceutica, St. Joseph, MO). A previously validated commercial rebound tonometer (TonoLab; Colonial Medical Supply, Franconia, NH) was used to take three sets of six measurements of IOP in each eye.[27,28] Right and left eye measurement sets were alternated with the initial eye selected randomly. All measurements were taken between 4 and 7 minutes after IP injection, because prior studies have shown this to be a period with stable IOP.[29,30] The rebound tonometer (TonoLab) was fixed horizontally for all measurements, and the tip of the probe was 2 to 3 mm from the eye. To reduce variability in measurements, the tonometer was modified to include a pedal that activated the probe without handling of the device. The probe contacted the eye perpendicularly over the central cornea. A set of measurements was accepted only if the device indicated that there was "no significant variability" (per instruction manual; Colonial Medical Supply). IOP measurements were taken between 11:00 AM and 3:00 PM.

Measurement of Central Corneal Thickness

In humans, Goldmann applanation tonometry may be affected by central corneal thickness (CCT). To assess whether this confounder is contributing to any observed IOP difference, CCTs of WT and TSP-null mice were measured using optical coherence tomography (OCT). As we have previously reported, mice were imaged with a Stratus OCT (Carl Zeiss Meditec, Inc., Dublin, CA) under anesthesia, and the process of locating the central corneal reflex was repeated three times to produce three different images.[19] CCT was obtained using the internal software (version 4.0.7; Carl Zeiss Meditec, Inc.) by measuring the peak-to-peak amplitude distance.

Assessment of Aqueous Humor Turnover

To investigate the mechanism of any IOP difference observed between WT and TSP-null mice, we noninvasively measured aqueous humor turnover using a previously published fluorophotometric technique.[19,31] In brief, all measurements were made between 11:00 AM and 3:00 PM to reduce potential variability related to diurnal variation of aqueous inflow or outflow. After anesthetizing each mouse with the same anesthesia mixture used for IOP measurement, 10 μL of 0.02% benzalkonium chloride (BAC) in saline was applied to the right eye to permeabilize the cornea to fluorescein.[32] After 5 minutes, the BAC solution was blotted at the lid margin without contacting the corneal epithelium and 10 μL of 0.02% fluorescein in saline was applied to the eye for 5 minutes. The eye and lids were then carefully washed with 600 μL of saline. The microscope was focused to a depth intermediate to the iris and cornea, and images were captured in 10-minute intervals thereafter for 1 hour (AxioCam ICC 1 camera and Stemi SV11 microscope, equipped with a GFP filter; Carl Zeiss Meditec, Inc.), using acquisition software (AxioVision, Release 4.6.3; Carl Zeiss Meditec, Inc.). Using ImageJ software (version 1.41; developed by Wayne Rasband, National Institutes of Health [NIH], Bethesda, MD; available at http://rsbweb.nih.gov/ij/download.html), an area with no corneal defects was selected and analyzed for average pixel intensity in the green channel. All averages were normalized to the intensity calculated for the image taken at time zero.

Light and Transmission Electron Microscopy

WT and TSP-null mice were euthanized with CO_2, and the eyes were enucleated for immediate fixation. An incision was made in the central cornea with a surgical blade (No. 11) to facilitate fixation. The globe was placed into fixative consisting of 2.5% gluteraldehyde and 2% formaldehyde in 0.1 M cacodylate buffer with 0.08 M $CaCl_2$ at 4°C for 24 hours, washed in 0.1 M cacodylate buffer, and postfixed for 1.5 hours in 2% aqueous osmium tetroxide. Tissue was dehydrated in graded concentrations of ethanol, transitioned in propylene oxide, infiltrated with propylene oxide and epon mixtures (TAAB 812 resin; Marivac, Quebec, Canada), embedded in epon, and cured for 48 hours at 60°C. Sections (1 μm) were cut (Leica Ultracut UCT; Leica Microsystems GmbH, Wetzlar, Germany) and stained with 1% toluidine blue in 1% borate buffer for light microscopy. Sections containing trabecular meshwork were then prepared for electron microscopy; thin sections (70 nm) were cut, stained with 4% uranyl acetate and lead citrate, and examined using a transmission electron microscope (JEM-

Table 1. The Primary Antibodies for Indirect Immunofluorescence

Primary Antibody	Dilution	Manufacturer
Mouse anti-mouse TSP1 IgG	1:100	NeoMarkers (Fremont, CA)
Mouse anti-mouse TSP2 IgG	1:100	BD Biosciences (San Jose, CA)

Table 2. Primer Sequences of Human TSP1, TSP2, and β-Actin Used for SYBR Green qPCR

	Forward	Reverse	Intron, Spanned
Thrombospondin-1, human	5′-TTGTCTTTGGAACCACACCA-3′	5′-CTGGACAGCTCATCACAGGA-3′	4
Thrombospondin-2, human	5′-TCGTGCGCTTTGACTACATC-3′	5′-GTGCCGTCAATCCAG AGGT-3′	4
β-Actin, human	5′-GGCATCCTCACCCTGAAGTA-3′	5′-GGGGTGTTGAAGGTCTCAAA-3′	3 and 4

1011; JEOL, Tokyo, Japan). Images were taken along Schlemm's canal (SC) at varying magnifications.

Measurement of Collagen Fibril Diameter

A single author was assigned to measure a total of 200 collagen fibril diameters from six TEM images from different locations of the JCT region for each eye at ×40,000 using ImageJ software (NIH). This author was masked with regard to the genotype of the eye from which the section was taken.

Indirect Immunofluorescence

Mouse eyes were enucleated and immediately prepared as above for fixation in 10% formalin for 24 hours. Sections (6 μm thick) from paraffin-embedded tissue were prepared from TSP1-null and their WT mouse eyes as well as TSP2-null and their WT mouse eyes. The sections were washed with xylene, hydrated with EtOH dilution (100%, 95%, and 70%), and rinsed with 1× PBS. After excess liquid was removed, 10% normal donkey serum in PBS was applied and incubated for 1 hour at room temperature. The tissues were permeabilized with 0.2% Triton X-100 in 1× PBS for 5 minutes. Primary antibodies were then applied to each section at 4°C overnight. Optimal primary antibody concentrations were empirically determined by serial antibody dilution (1:50 to 1:200). Secondary antibodies (1:200) were applied to detect target protein. Slides were washed three times with PBS/T for 10 minutes. Nuclei were stained in antifade reagent with DAPI (1:1) (SlowFade Gold; Invitrogen, Carlsbad, CA). Labeled tissues were analyzed with a spectral confocal laser scanning microscope (Leica TCS SP5; Leica Microsystems, Exton, PA). Primary antibodies to TSP1 and TSP2 were used (Table 1).

Cell Culture and Treatment with TGF-β2

Primary HTM endothelial cells were cultured from cadaveric donor anterior segments aged 42, 44, 45, 47, 62, 65, 70, and 74 years using a previously published protocol.[33] The cultures were maintained in Dulbecco's modified Eagle's medium (DMEM; Invitrogen) containing 20% fetal bovine serum, 1% L-glutamine (2 mM), and gentamycin (0.2 mg/mL) at 37°C in a 10% CO_2 atmosphere. All of the cell cultures were confluent passage 4 or passage 5 cultures that had been allowed to differentiate for 2 to 3 days.

TGF-β2 (R&D Systems, Minneapolis, MN) was reconstituted in 4 mM HCl solution containing 0.1% human serum albumin and added to HTM endothelial cell cultures at a dose of 2.5 ng/mL in serum-free media for 24 hours at 37°C. Control cells received 4 mM HCl solution containing 0.1% human serum albumin without TGF-β2 as a control. Total RNA and conditioned media were isolated from TGF-β2–treated HTM endothelial cells and analyzed via quantitative RT-PCR and immunoblot, respectively.

RNA Isolation and Quantitative RT-PCR

Total RNA from TM endothelial cells was isolated using a commercial reagent (TRIzol; Invitrogen). Briefly, harvested TM cell lysates were lysed with the commercial buffer (TRIzol), and chloroform was added. After centrifugation, total nucleic acid was isolated from the aqueous layer using ethanol precipitation. After digesting DNA by DNase I, total RNA was isolated and stored at −80°C.

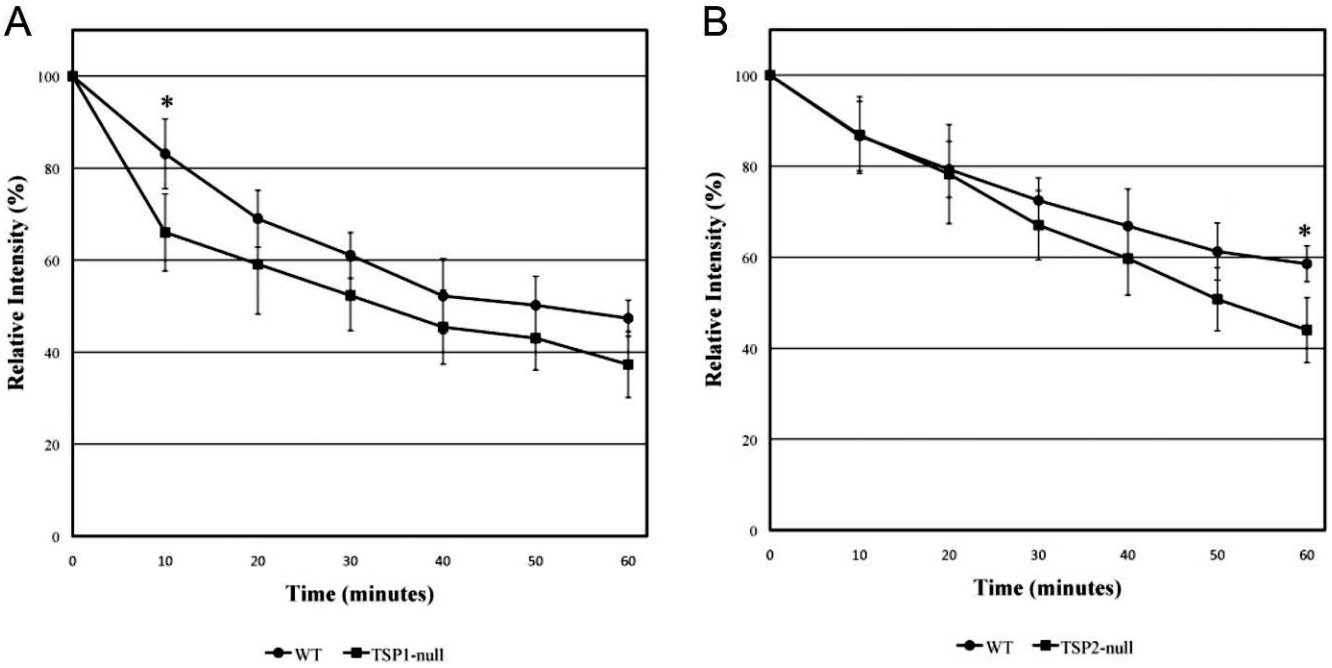

Figure 1. Average aqueous fluorescein intensity values are shown for (**A**) TSP1-null, (**B**) TSP2-null, and their corresponding WT mice. Least-squares fit for exponential decay yielded [% Intensity] = $100e^{-k \cdot \text{time}}$, with k values of 1.8% and 1.4% for TSP1-null and WT, and 1.3% and 1.0% for TSP2-null and WT mice, respectively. The *asterisk* indicates a significant difference in relative intensities ($P < 0.05$).

Table 3. Average TSP1-Null, TSP2-Null, and Their Corresponding WT Mice

Genotype	WT (*n*)	TSP-Null (*n*)	*P* Value
TSP1	15.8 ± 1.5 (68)	14.2 ± 2.0 (70)	10^{-7}
TSP2	18.1 ± 1.6 (54)	16.8 ± 2.0 (56)	10^{-4}

P values are calculated from Student's *t*-tests (*n* = eyes). Data showed mean ± SD.

Table 4. Average CCTs of TSP-Null and Corresponding WT Mice by OCT

Genotype	WT (*n*)	TSP-Null (*n*)	*P* Value
TSP1 (μm)	101.1 ± 4.5 (92)	94.5 ± 5.5 (57)	10^{-12}
TSP2 (μm)	103.9 ± 3.9 (60)	102.7 ± 2.9 (32)	0.12

Numbers of eyes are indicated (*n*). *P* values of *t*-tests are shown and were considered statistically significantly different for $P < 0.05$.

Complementary DNA (cDNA) was synthesized using a commercial kit (M-MLV RT kit; Promega, Madison, WI) according to the manufacturer's instructions with minor modifications. Briefly, 250 ng of total RNA was used as a template in 50 μL of reaction mixture including 250 ng of oligo-dT primer; 1× reaction buffer; 0.2 mM of dATG, dCTG, dGTG, dATG; 20 units of RNase inhibitor; and 200 units of M-MLV reverse transcriptase. The reaction mixture was incubated at 42°C for 1 hour and used for quantitative PCR (qPCR).

Quantitative reverse transcription–polymerase chain reaction (qRT-PCR) was performed to detect mRNA in cultured TM cells. Specific RNA messages were amplified in SYBR Green I master mix (Applied Biosystems Inc., Foster City, CA) using the real-time PCR system (AB StepOnePlus; Applied Biosystems). Quantification of the genes of interest was calculated by fold increase to β-actin expression using commercial software (Step One software v2.0; Applied Biosystems). All qPCR reactions were performed in triplicates. Primers for human TSP1, TSP2, and β-actin were designed using the Primer3 program (http://frodo.wi.mit.edu) spanning introns with an expected qPCR product of 200 bp[34] and are listed in Table 2.

Immunoblot Analysis

Conditioned media from TM cell cultures was removed and centrifuged at 2000*g* for 10 minutes at 4°C. The supernatant was collected, concentrated (Amicon Ultra-4 Filter Unit, 10 kDa; Millipore, Milford, MA), and protein content quantified (Bio-Rad DC Protein Assay; Bio-Rad, Hercules, CA). Equal amounts of protein were mixed with 2× reducing buffer (125 mM of Tris-HCl, pH 6.8, 4% SDS, 20% glycerol, 0.1% bromophenol blue with 5 mg/mL dithiothreitol [DTT]) and boiled for 5 minutes. Samples were then electrophoresed in 8% SDS-polyacrylamide gels, and proteins transferred to nitrocellulose membranes (0.45-μm pore size; Invitrogen). The membranes were incubated for 1 hour at

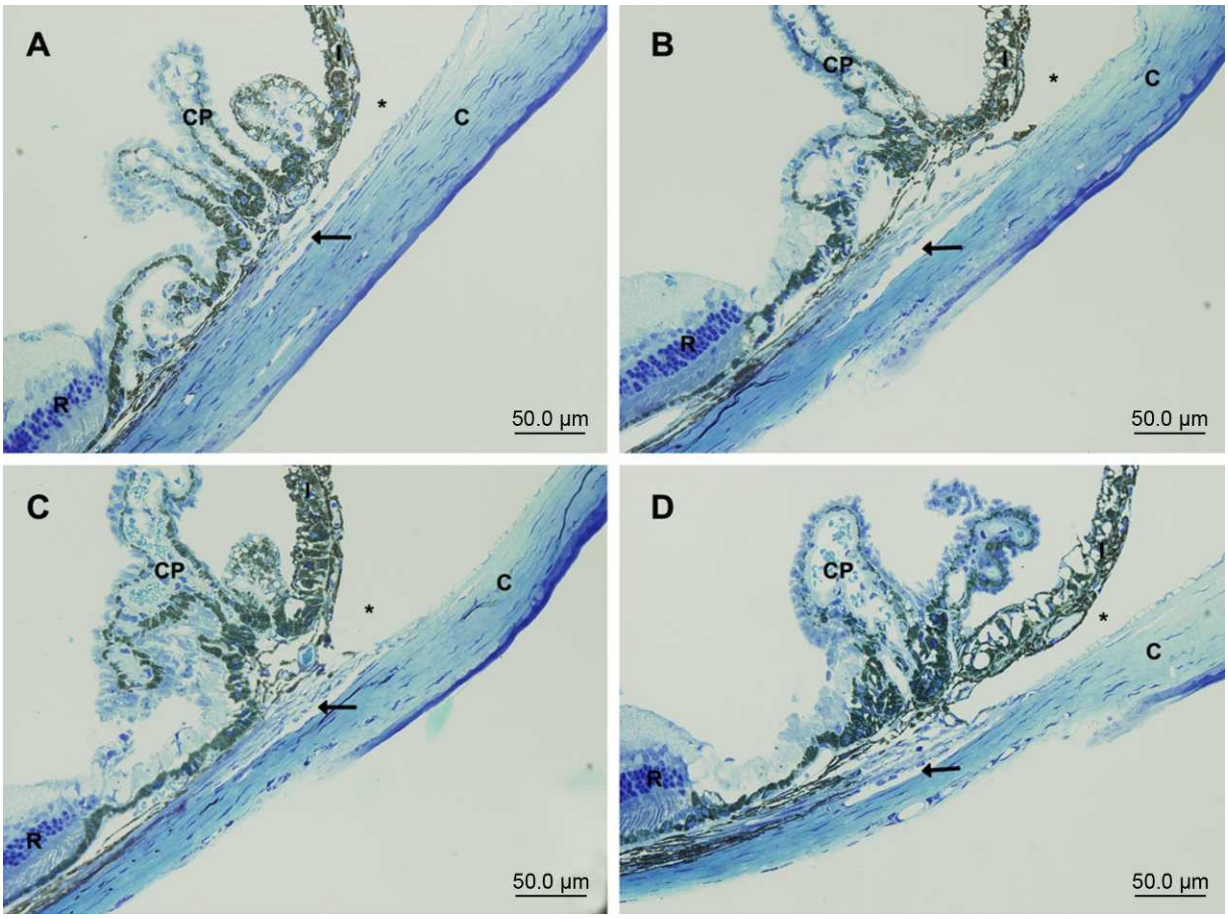

Figure 2. Light microscopy images of iridocorneal angles of TSP1-WT (**A**), TSP1-null (**B**), TSP2-WT (**C**), and TSP2-null (**D**) mice. Iridocorneal angles between TSP-WT and TSP-null mice appear grossly indistinguishable with similar Schlemm's canals, trabecular beams and cellularity, uveoscleral outflow pathway, and ciliary body location. Labels are as follows: ciliary processes (CP), anterior chamber (*), retina (R), cornea (C), iris (I), and Schlemm's canal and TM (*arrow*). *Scale bar*: −50 μm.

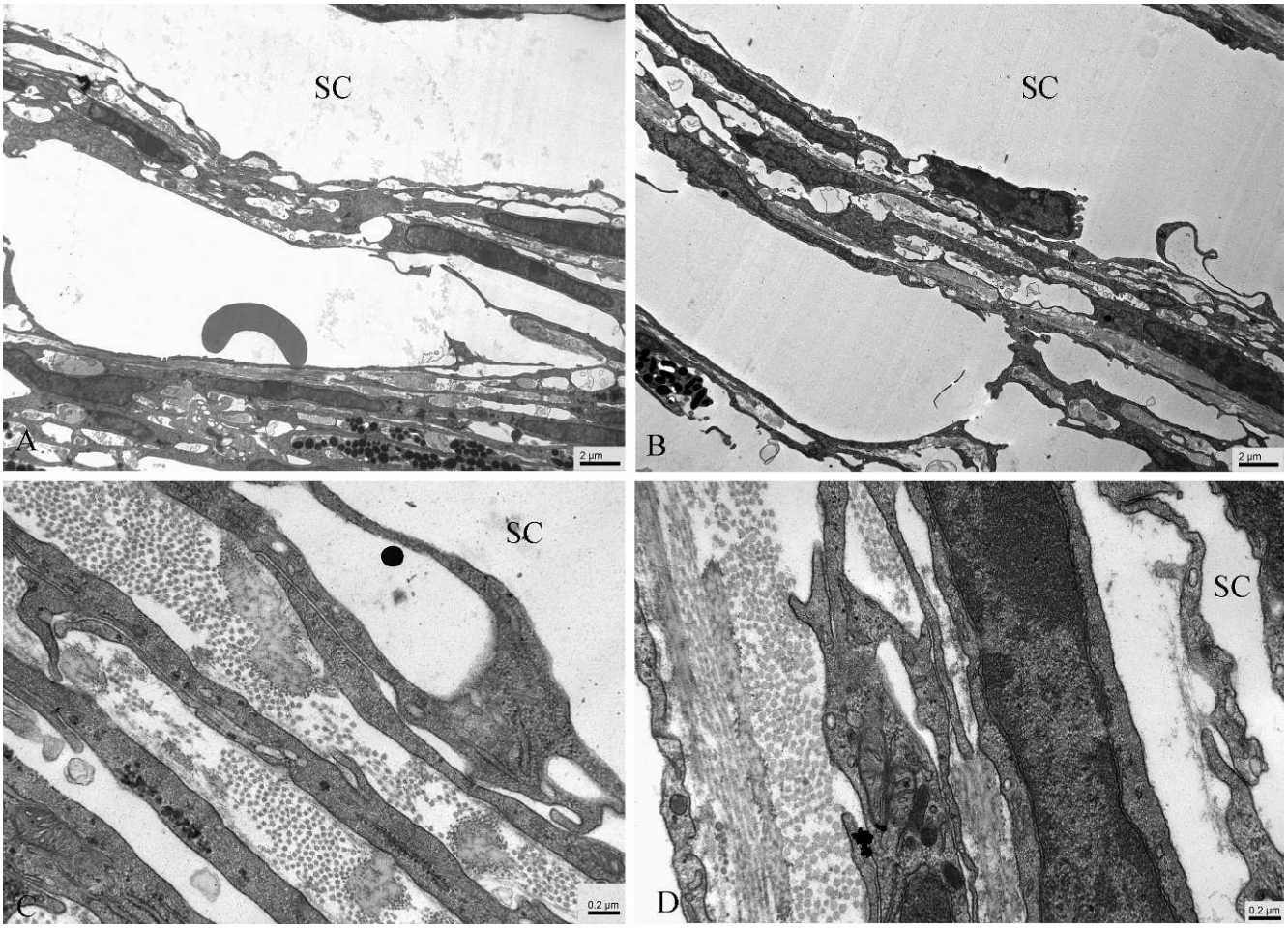

Figure 3. Low-magnification (×5000) transmission electron microscopy images of trabecular meshwork of TSP1-WT (**A**), TSP1-null (**B**) mice. The trabecular meshwork cellularity, trabecular beams, and appearance of extracellular matrix appear similar between TSP-WT and TSP-null mice. Quantitative measurements of collagen fibril diameters from high-magnification (×40,000) transmission electron microscopy images of trabecular meshwork of TSP1-WT (**C**), TSP1-null (**D**) mice revealed on average larger collagen fibril diameters in TSP1-WT mice. Schlemm's canal is labeled as SC. *Scale bar*: –2 μm for images (**A**) and (**B**), 0.2 μm for images (**C**) and (**D**).

room temperature in a 1:1 mixture of 1× TBS-T (20 mM Tris-HCl [pH 7.6], 137 mM NaCl, 0.1% Tween-20) and blocking buffer (Rockland Inc., Gilbertsville, PA), followed by an overnight incubation at 4°C with the respective primary antibody. The dilutions used for the primary antibodies were: 1:1000 for TSP1 (R&D Systems), 1:1000 for TSP2 (R&D Systems), and 1:2500 for GAPDH (Trevigen Inc., Gaithersburg, MD). Following antibody incubation, the membranes were washed three times with 1× TBS-T and incubated for 1 hour at room temperature with conjugated affinity purified anti-rabbit or anti-goat IgG antibodies (IRDye 800, 1:10,000 dilution; Rockland Inc.). The membranes were then washed three times with 1× TBS-T, scanned, and band densities were quantified (Odyssey Infrared Imaging System; Li-Cor, Lincoln, NE).

Statistics

IOP and CCT measurements of TSP-null and their corresponding WT mice were analyzed using Student's *t*-test. Aqueous humor turnover data were analyzed using a two-way repeated-measures ANOVA followed by all pairwise multiple comparison procedures (Student–Newman–Keuls method). Collagen fibril diameters of TSP-null and their corresponding WT mice were analyzed using the unpaired Student's *t*-test. The relative expressions of TSP1 and TSP2 after TGF-β2 incubation for 24 hours by qRT-PCR and immunoblot analyses were compared by paired Student's *t*-test. $P < 0.05$ was considered statistically significant.

Table 5. Average Collagen Fibril Diameters in the JCT of TM in TSP-Null and Corresponding WT Mice Measured by Transmission Electron Microscopy

	WT		TSP-Null		
Genotype	**Eye #1**	**Eye #2**	**Eye #1**	**Eye #2**	***P* Value**
TSP1, nm	37.3 ± 3.9	36.1 ± 3.5	44.7 ± 4.3	44.2 ± 4.4	0.03
TSP2, nm	37.4 ± 3.3	38.8 ± 3.9	43.0 ± 6.0	43.9 ± 5.3	0.03

The average for each eye represents 200 collagen fibril diameter measurements from a total of 6 sections. *P* values of *t*-tests are shown and were considered statistically significantly different ($P < 0.05$).

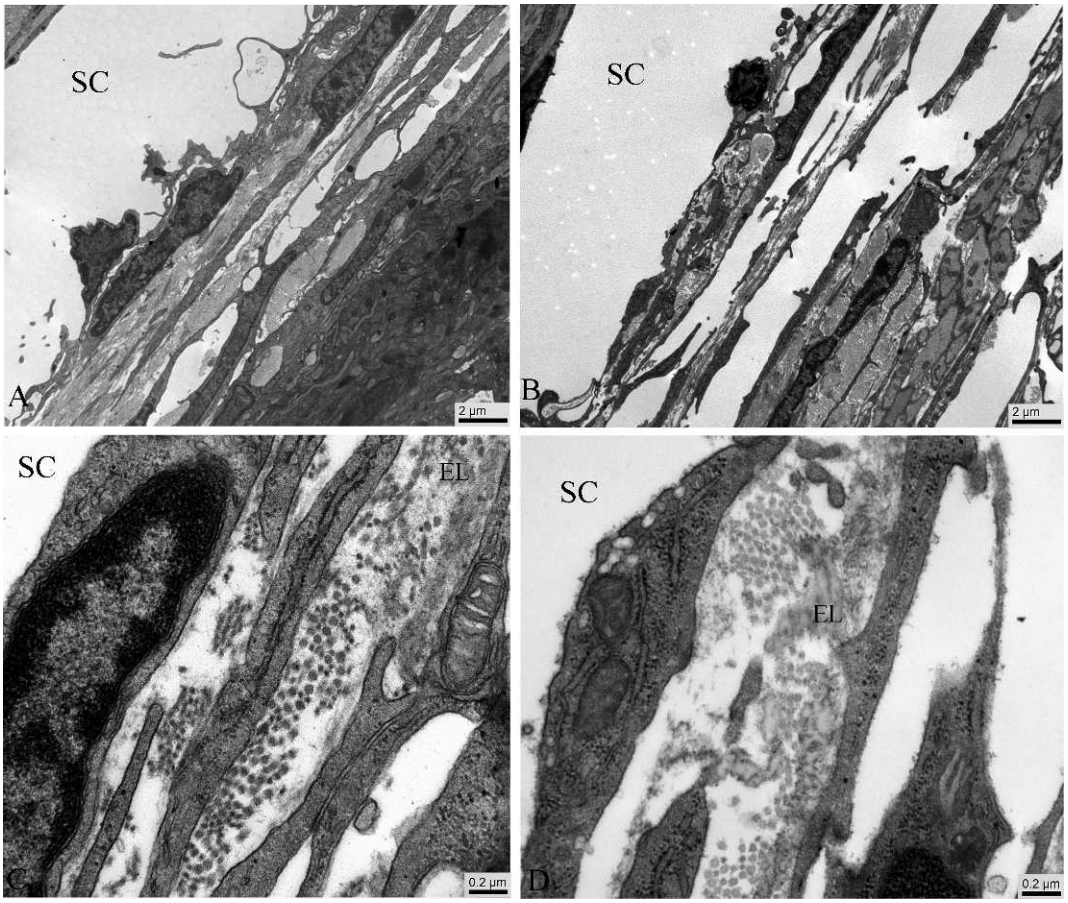

Figure 4. Low-magnification (×5000) transmission electron microscopy images of trabecular meshwork of TSP2-WT (**A**), TSP2-null (**B**) mice. The trabecular meshwork cellularity, trabecular beams, and appearance of extracellular matrix appear similar between TSP-WT and TSP-null mice. Quantitative measurements of collagen fibril diameters from high-magnification (×40,000) transmission electron microscopy images of trabecular meshwork of TSP2-WT (**C**), TSP2-null (**D**) mice revealed on average larger collagen fibril diameters in TSP2-WT mice. Schlemm's canal is labeled as SC. *Scale bar*: –2 μm for images (**A**) and (**B**), 0.2 μm for images (**C**) and (**D**).

Results

IOP

Average IOPs of TSP1-null and corresponding WT mice were 14.2 ± 2.0 and 15.8 ± 1.5 mm Hg, respectively (TSP1-null, $n =$ 70 eyes; WT, $n = 68$ eyes; Table 3). This 10% difference of IOP was statistically significantly different ($P < 0.05$). Average IOPs of TSP2-null and corresponding WT mice were 16.8 ± 2.0 and 18.1 ± 1.6 mm Hg, respectively (TSP2-null, $n = 56$ eyes; WT, $n = 54$ eyes; Table 3). The 7% difference in IOP was statistically significantly different ($P < 0.05$).

Central Corneal Thickness (CCT)

The CCTs of WT and TSP-null mice were measured by OCT (Table 4). Average CCTs measured by OCT were 101.1 ± 4.5 and 94.5 ± 5.5 μm for WT and TSP1-null mice, respectively ($P < 0.05$; $n = 92$ and 57 eyes, respectively). Average CCTs measured by OCT were 103.9 ± 3.9 and 102.7 ± 2.9 μm for WT and TSP2-null mice, respectively ($P > 0.05$; $n = 60$ and 32 eyes, respectively).

Assessment of Aqueous Humor Turnover

Least-squares fit analysis yielded exponential decay constants of 1.4%/min ($n = 5$ eyes; $r^2 = 0.93$) and 1.8%/min ($n = 5$ eyes; $r^2 = 0.83$) for WT and TSP1-null data, respectively (Fig. 1). Least-squares fit analysis yielded exponential decay constants of 1.0%/min ($n = 8$ eyes; $r^2 = 0.97$) and 1.3%/min ($n = 6$ eyes; $r^2 = 0.99$) for WT and TSP2-null data, respectively. Repeated-measures ANOVA comparison revealed significant differences in WT and TSP1-null values at the 10-minute time point ($P < 0.05$) but not at the 20, 30, 40, 50, and 60-minute time points ($P > 0.05$). Repeated-measures ANOVA comparison revealed significant difference in WT and TSP2-null values at the 60-minute time point ($P < 0.05$) but not at the 10, 20, 30, 40, and 50-minute time points ($P > 0.05$). Both TSP-null mice had turnover that was more rapid than that of their respective WTs ($P < 0.05$).

Light and Electron Microscopy

By light microscopy, the iridocorneal angles appear grossly indistinguishable with similar Schlemm canals, trabecular beams and cellularity, uveoscleral outflow pathway, and ciliary body location (Fig. 2).

By low-magnification transmission electron microscopy, the iridocorneal angles appear grossly indistinguishable with similar Schlemm canals, trabecular beams, and cellularity (Figs. 3, 4). Five mouse eyes from each of the four strains were examined and two eyes from each strain provided axial sections for which collagen fibril diameters could be measured. At high magnification, average collagen fibril diameters in the JCT were 36.7 ± 0.9 and 44.4 ± 0.4 nm for WT and TSP1-null

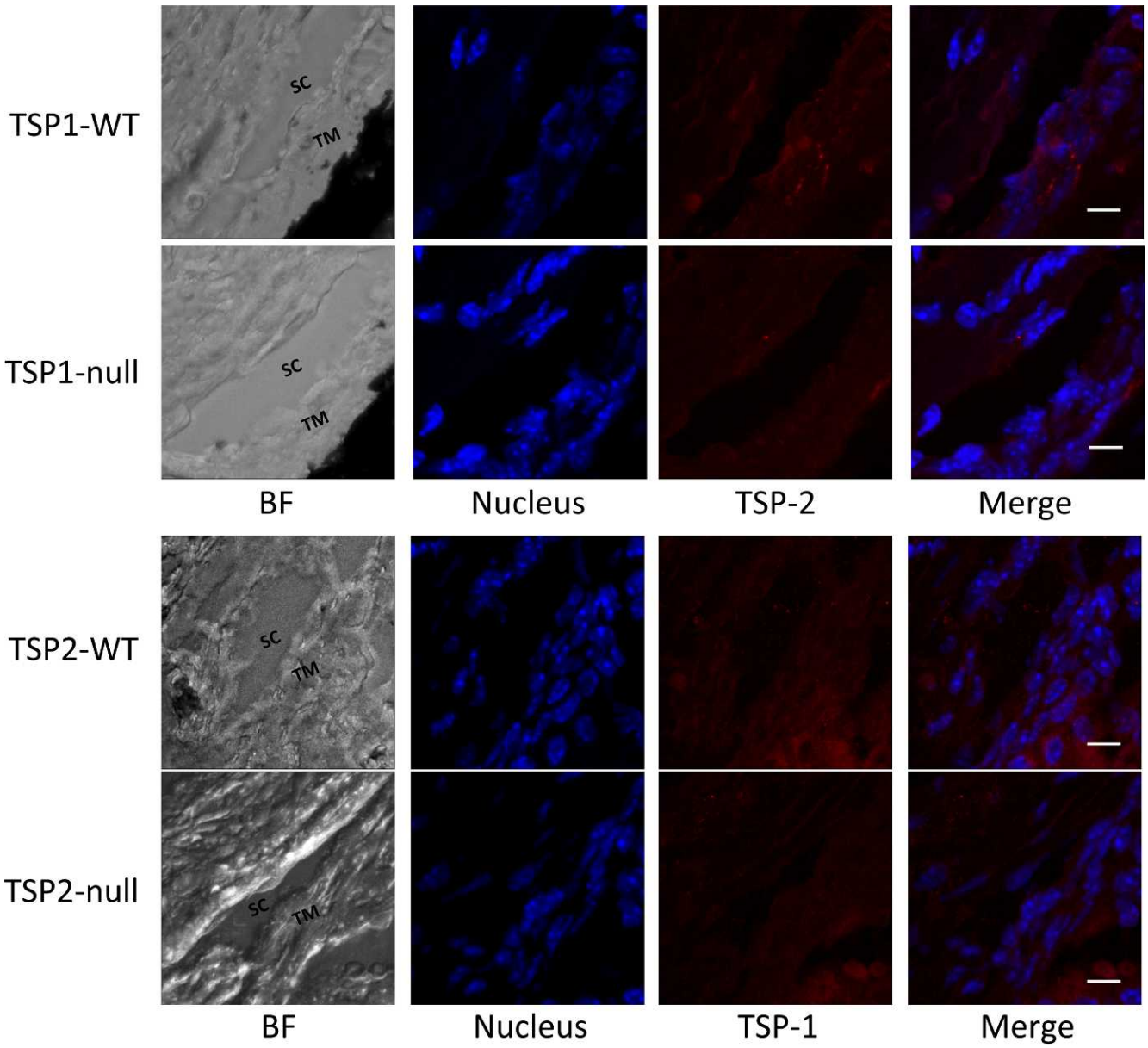

Figure 5. Immunofluorescence images of the TM and SC of TSP1-WT, TSP1-null, TSP2-WT, and TSP2-null mice are shown with corresponding images of bright field (BF) microscopy, DAPI stain, anti-TSP (1 or 2 as indicated), and merged images of DAPI and anti-TSP (*left* to *right*). There is qualitatively more diffuse staining of TSP2 in comparison with TSP1. Anti-TSP2 fluorescence appears reduced in TSP1-null mice compared with WT. Anti-TSP1 fluorescence appears reduced in TSP2-null mice compared with WT. *Scale bar*: −10 μm.

mice, respectively ($P = 0.03$; $n = 2$, respectively), and were 38.1 ± 1.0 and 43.5 ± 0.7 nm for WT and TSP2-null mice, respectively ($P = 0.03$; $n = 2$, respectively; Table 5).

Immunofluorescence

Five eyes from TSP1-null, TSP2-null, and their corresponding WTs were prepared for immunofluorescence imaging of the TM and SC (Fig. 5). Bright-field microscopy images were taken to orient DAPI and anti-TSP fluorescence anatomically. There is qualitatively more diffuse staining of TSP2 in comparison with TSP1. Anti-TSP2 fluorescence appears reduced in TSP1-null mice compared with WT. Anti-TSP1 fluorescence appears reduced in TSP2-null mice compared with WT.

Relative Expression of TSP1 and TSP2 following TGF-β2 Incubation

Following TGF-β2 incubation, TM cells showed increases in TSP1 and TSP2 mRNA levels by 14.50-fold and 9.64-fold, with TSP1 levels reaching statistical significance ($P < 0.05$, Fig. 6A). Immunoblot assays showed increases in TSP1 and TSP2 protein levels by 3.44-fold and 1.37-fold, with TSP1 levels reaching statistical significance ($P < 0.05$, Fig. 6B).

Discussion

TSP1-null and TSP2-null mice have lower IOPs than their corresponding WT mice. To investigate the possibility of artifactual differences in rebound tonometry IOP readings,

A

	Control (6)	TGF-β2 treatment (6)	p-value
TSP-1	1.00 ± 00	14.50 ± 6.00	0.009
TSP-2	1.00 ± 00	9.64 ± 4.87	0.163

B

	Control (6)	TGF-β2 treatment (6)	p-value
TSP-1	1.00 ± 00	3.44 ± 0.46	0.013
TSP-2	1.00 ± 00	1.37 ± 0.16	0.106

C

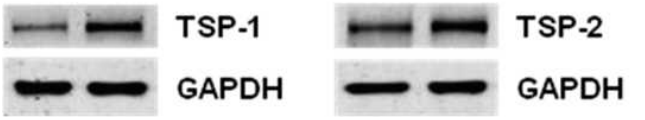

Figure 6. Relative expression of TSP1 and TSP2 after TGF-β2 incubation for 24 hours by (**A**) qRT-PCR ($n = 6$ for control and treatment groups) and (**B**) by immunoblot analyses ($n = 6$ for control and treatment groups). Data showed mean ± SD and were analyzed by paired Student's *t*-test. Representative immunoblots of TSP1 and TSP2 from conditioned media after TGF-β2 incubation for 24 hours are shown in (**C**) with control samples on the *left* and TGF-β2–treated samples on the *right*.

CCT was measured using OCT. Our average CCT measurements are consistent with previously reported ranges.[19,35] CCTs of WT mice tended to be slightly thicker; however, the largest difference between strains was 6.5%, which would be unlikely to account for any significant differences in corneal biomechanics. Mice demonstrate strain-dependent differences in CCT. Additionally, the rebound tonometer has been previously validated not only by our group but also by other groups across numerous strains, not requiring specific calibrations for each strain.[19,27,28] Furthermore, impact rebound tonometry does not seem to be subject to CCT.[36,37]

We found that our TSP-null mice had an increased rate of dye disappearance from the anterior chamber. This observation could be the result of two mechanisms: increased aqueous production or decreased resistance in aqueous outflow pathways. In the setting of a lower IOP, decreased outflow resistance must be present even if there is increased aqueous production. Thus, our data implicate that the mechanism of lower IOP is enhanced aqueous drainage.

At the light microscopy level, we did not find structural differences between TSP1-null and WT mice iridocorneal angles. Both conventional and uveoscleral outflow pathways have been identified in the mouse.[38] Immunohistochemistry identified expression of both TSP1 and TSP2 in WT mice. In humans, TSP1 is expressed throughout the TM, with a predominance in the JCT region, whereas TSP2 is more concentrated in the uveal meshwork.[14] Such localization is difficult in the mouse because there are fewer cellular layers of TM, and therefore the tissue is more susceptible to morphologic processing artifact. The expression levels of TSP1 and TSP2 in the TM of TSP2-null and TSP1-null mice were also investigated to determine whether there is compensatory overexpression or corresponding underexpression of the other TSP subgroup A protein. Although only a qualitative result, the immunofluorescence suggests that TSP1-null mice have reduced expression of TSP2 and, similarly, TSP2-null mice have reduced expression of TSP1. Bornstein et al.[39] summarize their studies of TSP1 and TSP2 with regard to cell–matrix interactions, and indicate different spatial and temporal expression patterns for the two genes, which are consistent with significant differences in their promoter sequences. They have not observed a compensatory increase in expression of the paralogous TSP gene in either TSP knockout mouse. Our qualitative findings suggest the contrary, that there may be a synergistic effect for expression of TSP1 and TSP2. Study of a TSP1–TSP2 double-knockout mouse may help further clarify these results. If the IOP of such a mouse is not reduced more than that in the individual knockout models, this may support our qualitative finding that the paralogous TSP expression is already reduced in a single knockout model.

Although the iridocorneal angles appear indistinguishable at the light microscopy level as well as with low-magnification electron microscopy, quantitative analysis of collagen fibril diameter by electron microscopy of the JCT reveals significantly increased diameters in both TSP-null mice. In the initial characterization of the TSP2-null mouse, Kyriakides et al.[25] described larger and more irregularly contoured collagen fibrils. This was described in conjunction with reduced tensile strength of TSP2-null skin compared with WT. To date, no one has reported electron microscopic evaluation of collagen fibrils in TSP1-null mice. Histologic examination has identified a paucity of dermal matrix.[21] The roles of TSP1 and TSP2 in cell–matrix interactions have been well described. TSP1 suppressed activation of promatrix metalloproteinase (MMP)9, and TSP-null mice exhibit higher levels of activated MMP9.[40] TSP2 binding to MMP2 and internalizing on a common receptor has been proposed as a regulatory mechanism for extracellular MMP2 levels.[41] Moreover, TSP2-null mice exhibit significantly greater MMP2 levels.[42] Enlarged collagen fibril diameter in the JCT of TSP1-null and TSP2-null mice may be either a direct or indirect sign of altered matrix turnover, which in turn may affect outflow facility.

The availability of transgenic mice has provided a valid and useful model for the study of glaucoma and IOP regulation.[43] Many, but not all, of the matricellular family seem to have an important role in IOP regulation, but the exact mechanisms by which they exert their effect are unknown. The transgenic deletion of osteopontin and hevin do not have an effect on IOP.[37,44] We have previously shown that SPARC, which is highly expressed in TM, and SPARC-null mice have decreased IOP and decreased aqueous outflow resistance.[19] SPARC is located within a known locus, 5q22.1-q32 (GLC1M), for juvenile open-angle glaucoma, although no mutation, polymorphism, or copy number variation has been identified that correlates with the family from which GLC1M has been described.[45] TSP1 expression within the trabecular meshwork is increased in one third of patients with primary open-angle glaucoma (POAG).[16] TSP1 has also been found to be intimately related to TGF-1 and TGF-2. TGF-2 is increased in the aqueous humor of patients with POAG and, in experimental model systems, TGF-2 elevates IOP and induces changes within the trabecular meshwork ECM.[46–54] Expression within the JCT region and relationship between TGF-2 and matricellular proteins may be important. Both SPARC and TSP1 are expressed within the JCT region and their expression by human trabecular meshwork cells is upregulated by TGF-2.[44]

TSP2 levels do not respond to TGF-2. Nevertheless, TSP2-null mice have an altered IOP. This is perhaps consistent with the findings that TSP1 and TGF-1–null mice exhibit markedly similar histopathologic changes in numerous organ systems. Pathologic findings in TSP1-null mice were corrected by the addition of the TSP1-derived peptide that activates TGF-1.[21] As stated previously, TSP1 also alters MMP expression. On the other hand, TSP2-null mice alter MMP levels but do not alter TGF-1 levels.[42] The two TSP proteins in subgroup A may therefore both alter outflow facility by different but overlapping mechanisms. Further study would be warranted to elucidate these mechanisms.

Our findings suggest that subgroup A TSPs (TSP1 and TSP2) are involved in aqueous outflow resistance. Our morphologic studies suggest that there is alteration of the ECM in the JCT region; however, the precise mechanism remains elusive. In the future, the treatments developed to reduce levels of thrombospondins or other matricellular proteins may offer alternative therapies for glaucoma.

Acknowledgments

The authors thank Jarema Malicki, PhD, of the Howe Lab for his generosity with imaging equipment for the aqueous humor turnover study.

References

1. Resnikoff S, Pascolini D, Etya'ale D, et al. Global data on visual impairment in the year 2002. *Bull World Health Organ*. 2004; 82:844–851.
2. Grant WM. Experimental aqueous perfusion in enucleated human eyes. *Arch Ophthalmol*. 1963;69:783–801.
3. Bradley JM, Vranka J, Colvis CM, et al. Effect of matrix metalloproteinases activity on outflow in perfused human organ culture. *Invest Ophthalmol Vis Sci*. 1998;39:2649–2658.
4. Oh DJ, Martin JL, Williams AJ, Russell P, Birk DE, Rhee DJ. Effect of latanoprost on the expression of matrix metalloproteinases and their tissue inhibitors in human trabecular meshwork cells. *Invest Ophthalmol Vis Sci*. 2006;47:3887–3895.
5. Pang IH, Hellberg PE, Fleenor DL, Jacobson N, Clark AF. Expression of matrix metalloproteinases and their inhibitors in human trabecular meshwork cells. *Invest Ophthalmol Vis Sci*. 2003;44:3485–3493.
6. Bornstein P, Sage EH. Matricellular proteins: extracellular modulators of cell function. *Curr Opin Cell Biol*. 2002;14: 608–616.
7. Rhee DJ, Haddadin RI, Kang MH, Oh DJ. Matricellular proteins in the trabecular meshwork. *Exp Eye Res*. 2008;88:694–703.
8. Yan Q, Sage EH. SPARC, a matricellular glycoprotein with important biological functions. *J Histochem Cytochem*. 1999; 47:1495–1506.
9. Yan Q, Clark JI, Sage EH. Expression and characterization of SPARC in human lens and in the aqueous and vitreous humors. *Exp Eye Res*. 2000;71:81–90.
10. Berryhill BL, Kane B, Stramer BM, Fini ME, Hassell JR. Increased SPARC accumulation during corneal repair. *Exp Eye Res*. 2003;77:85–92.
11. Kantorow M, Huang Q, Yang XJ, et al. Increased expression of osteonectin/SPARC mRNA and protein in age-related human cataracts and spatial expression in the normal human lens. *Mol Vis*. 2000;6:24–29.
12. Rhee DJ, Fariss RN, Brekken R, Sage EH, Russell P. The matricellular protein SPARC is expressed in human trabecular meshwork. *Exp Eye Res*. 2003;77:601–607.
13. Gilbert RE, Cox AJ, Kelly DJ, et al. Localization of secreted protein acidic and rich in cysteine (SPARC) expression in the rat eye. *Connect Tissue Res*. 1999;40:295–303.
14. Hiscott P, Paraoan L, Choudhary A, Ordonez JL, Al-Khaier A, Armstrong DJ. Thrombospondin 1, thrombospondin 2 and the eye. *Prog Retin Eye Res*. 2006;25:1–18.
15. Tomarev SI, Wistow G, Raymond V, Dubois S, Malyukova I. Gene expression profile of the human trabecular meshwork: NEIBank sequence tag analysis. *Invest Ophthalmol Vis Sci*. 2003;44:2588–2596.
16. Flugel-Koch C, Ohlmann A, Fuchshofer R, Welge-Lussen U, Tamm ER. Thrombospondin-1 in the trabecular meshwork: localization in normal and glaucomatous eyes, and induction by TGF-beta1 and dexamethasone in vitro. *Exp Eye Res*. 2004; 79:649–663.
17. Suzuki K, Wang R, Kubota H, Shibuya H, Saegusa J, Sato T. Kinetics of biglycan, decorin and thrombospondin-1 in mercuric chloride-induced renal tubulointerstitial fibrosis. *Exp Mol Pathol*. 2005;79:68–73.
18. Uno K, Hayashi H, Kuroki M, Uchida H, Yamauchi Y, Oshima K. Thrombospondin-1 accelerates wound healing of corneal epithelia. *Biochem Biophys Res Commun*. 2004;315:928–934.
19. Haddadin RI, Oh DJ, Kang MH, et al. SPARC-null mice exhibit lower intraocular pressures. *Invest Ophthalmol Vis Sci*. 2009; 50:3771–3777.
20. Vittal V, Rose A, Gregory KE, Kelley MJ, Acott TS. Changes in gene expression by trabecular meshwork cells in response to mechanical stretching. *Invest Ophthalmol Vis Sci*. 2005;46: 2857–2868.
21. Crawford SE, Stellmach V, Murphy-Ullrich JE, et al. Thrombospondin-1 is a major activator of TGF-beta1 in vivo. *Cell*. 1998; 93:1159–1170.
22. Adams JC, Lawler J. The thrombospondins. *Int J Biochem Cell Biol*. 2004;36:961–968.
23. Hankenson KD, Bain SD, Kyriakides TR, Smith EA, Goldstein SA, Bornstein P. Increased marrow-derived osteoprogenitor cells and endosteal bone formation in mice lacking thrombospondin 2. *J Bone Miner Res*. 2000;15:851–862.
24. Kyriakides TR, Tam JW, Bornstein P. Accelerated wound healing in mice with a disruption of the thrombospondin 2 gene. *J Invest Dermatol*. 1999;113:782–787.
25. Kyriakides TR, Zhu YH, Smith LT, et al. Mice that lack thrombospondin 2 display connective tissue abnormalities that are associated with disordered collagen fibrillogenesis, an increased vascular density, and a bleeding diathesis. *J Cell Biol*. 1998;140:419–430.
26. Lawler J, Sunday M, Thibert V, et al. Thrombospondin-1 is required for normal murine pulmonary homeostasis and its absence causes pneumonia. *J Clin Invest*. 1998;101:982–992.
27. Wang WH, Millar JC, Pang IH, Wax MB, Clark AF. Noninvasive measurement of rodent intraocular pressure with a rebound tonometer. *Invest Ophthalmol Vis Sci*. 2005;46:4617–4621.
28. Saeki T, Aihara M, Ohashi M, Araie M. The efficacy of TonoLab in detecting physiological and pharmacological changes of mouse intraocular pressure—comparison with TonoPen and microneedle manometery. *Curr Eye Res*. 2008;33:247–252.
29. Aihara M, Lindsey JD, Weinreb RN. Reduction of intraocular pressure in mouse eyes treated with latanoprost. *Invest Ophthalmol Vis Sci*. 2002;43:146–150.
30. Savinova OV, Sugiyama F, Martin JE, et al. Intraocular pressure in genetically distinct mice: an update and strain survey. *BMC Genet*. 2001;2:Art. 12.
31. Avila MY, Mitchell CH, Stone RA, Civan MM. Noninvasive assessment of aqueous humor turnover in the mouse eye. *Invest Ophthalmol Vis Sci*. 2003;44:722–727.

32. Burstein NL. Preservative alteration of corneal permeability in humans and rabbits. *Invest Ophthalmol Vis Sci*. 1984;25: 1453–1457.
33. Stamer WD, Seftor RE, Williams SK, Samaha HA, Snyder RW. Isolation and culture of human trabecular meshwork cells by extracellular matrix digestion. *Curr Eye Res*. 1995;14:611–617.
34. Rozen S, Skaletsky HJ. Primer3 on the WWW for general users and for biologist programmers. In: Krawetz S, Misener S, eds. *Bioinformatics Methods and Protocols: Methods in Molecular Biology*. Totowa, NJ: Humana Press; 2000:365–386.
35. Schulz D, Iliev ME, Frueh BE, Goldblum D. In vivo pachymetry in normal eyes of rats, mice and rabbits with the optical low coherence reflectometer. *Vision Res*. 2003;43:723–728.
36. Nissirios N, Goldblum D, Rohrer K, Mittag T, Danias J. Noninvasive determination of intraocular pressure (IOP) in nonsedated mice of 5 different inbred strains. *J Glaucoma*. 2007;16:57–61.
37. Chowdhury UR, Jea SY, Oh DJ, Rhee DJ, Fautsch MP. Expression profile of the matricellular protein osteopontin in primary open-angle glaucoma and the normal human eye. *Invest Ophthalmol Vis Sci*. 2011;52:6443–6451.
38. Lindsey JD, Weinreb RN. Identification of the mouse uveoscleral outflow pathway using fluorescent dextran. *Invest Ophthalmol Vis Sci*. 2002;43:2201–2205.
39. Bornstein P, Agah A, Kyriakides TR. The role of thrombospondins 1 and 2 in the regulation of cell-matrix interactions, collagen fibril formation, and the response to injury. *Int J Biochem Cell Biol*. 2004;36:1115–1125.
40. Rodriguez-Manzaneque JC, Lane TF, Ortega MA, Hynes RO, Lawler J, Iruela-Arispe ML. Thrombospondin-1 suppresses spontaneous tumor growth and inhibits activation of matrix metalloproteinase-9 and mobilization of vascular endothelial growth factor. *Proc Natl Acad Sci USA*. 2001;98:12485–12490.
41. Yang Z, Strickland DK, Bornstein P. Extracellular matrix metalloproteinase 2 levels are regulated by the low density lipoprotein-related scavenger receptor and thrombospondin 2. *J Biol Chem*. 2001;276:8403–8408.
42. Kyriakides TR, Zhu YH, Yang Z, Huynh G, Bornstein P. Altered extracellular matrix remodeling and angiogenesis in sponge granulomas of thrombospondin 2-null mice. *Am J Pathol*. 2001;159:1255–1262.
43. Lindsey JD, Weinreb RN. Elevated intraocular pressure and transgenic applications in the mouse. *J Glaucoma*. 2005;14: 318–320.
44. Kang MH, Oh DJ, Rhee DJ. Effect of hevin deletion in mice and characterization in trabecular meshwork. *Invest Ophthalmol Vis Sci*. 2011;52:2187–2193.
45. Rozsa FW, Reed DM, Scott KM, et al. Gene expression profile of human trabecular meshwork cells in response to long-term dexamethasone exposure. *Mol Vis*. 2006;12:125–141.
46. Tripathi RC, Li J, Chan WF, Tripathi BJ. Aqueous humor in glaucomatous eyes contains an increased level of TGF-beta 2. *Exp Eye Res*. 1994;59:723–727.
47. Picht G, Welge-Luessen U, Grehn F, Lutjen-Drecoll E. Transforming growth factor beta 2 levels in the aqueous humor in different types of glaucoma and the relation to filtering bleb development. *Graefes Arch Clin Exp Ophthalmol*. 2001;239: 199–207.
48. Ochiai Y, Ochiai H. Higher concentration of transforming growth factor-beta in aqueous humor of glaucomatous eyes and diabetic eyes. *Jpn J Ophthalmol*. 2002;46:249–253.
49. Ozcan AA, Ozdemir N, Canataroglu A. The aqueous levels of TGF-beta2 in patients with glaucoma. *Int Ophthalmol*. 2004; 25:19–22.
50. Fuchshofer R, Welge-Lussen U, Lutjen-Drecoll E. The effect of TGF-beta2 on human trabecular meshwork extracellular proteolytic system. *Exp Eye Res*. 2003;77:757–765.
51. Zhao X, Ramsey KE, Stephan DA, Russell P. Gene and protein expression changes in human trabecular meshwork cells treated with transforming growth factor-beta. *Invest Ophthalmol Vis Sci*. 2004;45:4023–4034.
52. Wordinger RJ, Fleenor DL, Hellberg PE, et al. Effects of TGF-beta2, BMP-4, and gremlin in the trabecular meshwork: implications for glaucoma. *Invest Ophthalmol Vis Sci*. 2007; 48:1191–1200.
53. Gottanka J, Chan D, Eichhorn M, Lutjen-Drecoll E, Ethier CR. Effects of TGF-beta2 in perfused human eyes. *Invest Ophthalmol Vis Sci*. 2004;45:153–158.
54. Fleenor DL, Shepard AR, Hellberg PE, Jacobson N, Pang IH, Clark AF. TGFbeta2-induced changes in human trabecular meshwork: implications for intraocular pressure. *Invest Ophthalmol Vis Sci*. 2006;47:226–234.